

Quantum simulation of strong Charge-Parity violation and Peccei-Quinn mechanism

Le Bin Ho^{1,2,*}

¹Frontier Research Institute for Interdisciplinary Sciences, Tohoku University, Sendai 980-8578, Japan

²Department of Applied Physics, Graduate School of Engineering, Tohoku University, Sendai 980-8579, Japan

(Dated: January 14, 2026)

Quantum Chromodynamics (QCD) admits a topological $\bar{\theta}$ -term that violates Charge-Parity (CP) symmetry, yet experimental indicate that $\bar{\theta}$ is nearly zero. To investigate this discrepancy in a controlled setting, we derive the Hamiltonian representation of the QCD Lagrangian and construct its (1+1)-dimensional Schwinger-model analogue. By encoding fermionic and gauge degrees of freedom into qubits using the Jordan-Wigner and quantum-link schemes, we obtain a compact Pauli Hamiltonian that retains the relevant topological vacuum structure. Ground states are evaluated using a feedback-based quantum optimization protocol, enabling numerical evaluation of the vacuum energy $E_0(\bar{\theta})$ on a few-qubit simulator. Our results show a vacuum at $\bar{\theta} = 0 \pmod{2}$ in agreement with strong-interaction expectations, and demonstrate that introducing a dynamical axion field drives the system toward a $\theta_{\text{eff}} = 0$, thereby realizing the Peccei-Quinn mechanism within a minimal quantum simulation. These results illustrate how quantum hardware can examine symmetry violation and its dynamical resolution in gauge theories.

Introduction. Quantum chromodynamics (QCD) is an $SU(3)$ non-Abelian gauge theory describing the interactions of quarks and gluons [1–3]. In addition to the standard kinetic and interaction terms [3], the QCD action admits a topological term associated with gauge-field configurations of nontrivial winding number. This term is odd under charge-parity (CP) transformations and leads to explicit CP violation when its coefficient is nonzero [4, 5]. Although this term does not affect perturbative processes, it plays a central role in shaping the nonperturbative vacuum structure of the theory [6]. Including this contribution, the QCD Lagrangian can be written as

$$\mathcal{L}_{\text{QCD}} = -\frac{1}{4}G_{\mu\nu}^a G^{a,\mu\nu} + \sum_f \bar{\psi}_f (i\gamma^\mu D_\mu - m_f) \psi_f + \bar{\theta} \frac{g^2}{32\pi^2} G_{\mu\nu}^a \tilde{G}^{a,\mu\nu}. \quad (1)$$

Here $G_{\mu\nu}^a = \partial_\mu A_\nu^a - \partial_\nu A_\mu^a + g f^{abc} A_\mu^b A_\nu^c$ denotes the gluon field-strength tensor, and $\tilde{G}^{a,\mu\nu} = \frac{1}{2}\epsilon^{\mu\nu\rho\sigma} G_{\rho\sigma}^a$ its dual, where A_μ^a are the gluon gauge fields and f^{abc} are the structure constants of the $SU(3)$ Lie algebra. The quark field of flavor f is denoted by ψ_f and carries mass m_f . Its interaction with the gluon field is described by the gauge-covariant derivative $D_\mu = \partial_\mu - ig T^a A_\mu^a$, where g is the strong coupling constant and T^a are the generators of the $SU(3)$ color group, satisfying the commutation relations $[T^a, T^b] = if^{abc}T^c$.

Because the QCD gauge field admits topologically nontrivial configurations, the most general gauge-invariant action allows a term proportional to $G_{\mu\nu}^a \tilde{G}^{a,\mu\nu}$. Its coefficient θ is the QCD vacuum angle and controls explicit CP violation. When the quark mass matrix M carries complex phases, an anomalous axial $U(1)_A$ rotation shifts these phases into the topological term. As a result, the physically observable CP -violating parameter is $\bar{\theta} = \theta - \text{argdet}(M)$, where M denotes the full quark

mass matrix. Since $G_{\mu\nu}^a \tilde{G}^{a,\mu\nu}$ is odd under CP , QCD is CP -symmetric only when $\bar{\theta} = 0$, any nonzero value of $\bar{\theta}$ therefore leads to explicit CP violation.

In QCD, such a violation would be expected to generate low-energy hadronic effects. For example, it induces a permanent electric dipole moment (EDM) of the neutron [7, 8]. Precision measurements, however, have not observed such a signal. The current experimental bound places the neutron EDM $|d_n| < 1.8 \times 10^{-26} e \cdot \text{cm}$ (90% C.L.) [9, 10], which implies an extraordinarily small value of $|\bar{\theta}| \lesssim 10^{-10}$. This extreme suppression cannot be explained within the Standard Model, leading to the strong CP problem: QCD allows a large $\bar{\theta}$, yet nature appears to choose a value extremely close to zero.

A compelling theoretical resolution is provided by the Peccei-Quinn mechanism [6, 11–13], which promotes $\bar{\theta}$ to a dynamical field associated with a spontaneously broken global $U(1)_{\text{PQ}}$ symmetry. The resulting pseudo-Nambu-Goldstone boson, known as the axion, dynamically relaxes the effective $\bar{\theta}$ parameter to zero, thereby restoring CP symmetry in the strong interactions [6]. The axion $a(x)$ couples anomalously to gluons

$$\mathcal{L}_a = \frac{g^2}{32\pi^2} \frac{a}{f_a} G_{\mu\nu}^a \tilde{G}^{a,\mu\nu}, \quad (2)$$

where f_a is the decay constant. As a result, the effective CP -violating angle becomes $\theta_{\text{eff}} = \theta + \frac{a}{f_a}$. Non-perturbative QCD dynamics generate an effective potential $V(\theta_{\text{eff}})$ for this combination, which guarantee that the vacuum energy is minimized at $\theta_{\text{eff}} = 0$ independent of microscopic details. Consequently, the axion acquires a vacuum expectation value $\langle a \rangle = -\bar{\theta}f_a$ dynamically canceling the CP -violating phase. After shifting $a = a_{\text{phys}} + \langle a \rangle$, the QCD vacuum is exactly CP -symmetric, while the physical axion a_{phys} remains as a light excitation around the minimum. In this way, the Peccei-Quinn mechanism does not rely on fine-tuning or

an exact symmetry of the Standard Model. Instead, CP conservation in the strong sector emerges dynamically from vacuum alignment, with the axion providing the necessary degree of freedom. The axion framework not only resolves the strong CP problem but also provides a well-motivated candidate for dark matter, linking fundamental particle physics with cosmological observations [14].

Theoretical progress on the strong- CP problem is limited by the fact that the QCD vacuum is intrinsically nonperturbative and difficult to treat with conventional techniques. Conventional lattice methods struggle with real-time dynamics and $\bar{\theta}$ -dependence, while analytical techniques rely on approximations. Quantum simulation [15, 16] provides a complementary route: instead of performing numerical sampling, one implements a controllable quantum system whose Hilbert space directly encodes the gauge theory and then measures how its vacuum responds to a CP -violating background. The (1+1)-dimensional Schwinger model retains essential features such as confinement and topological vacuum sectors, yet is sufficiently simple to be mapped to a small number of qubits and executed on near-term hardware.

In this work, we use the (1+1)-dimensional Schwinger model to examine the microscopic origin of strong CP violation and its axionic restoration. We construct a qubit-encoded Schwinger model with a $\bar{\theta}$ -dependent electric sector, extend it to include a dynamical axion field, and prepare its vacuum using a feedback-driven quantum optimization algorithm (FALQON) [17]. By computing the vacuum energy as a function of $\bar{\theta}$, we first characterize the $\bar{\theta}$ -dependent vacuum structure of the lattice gauge theory in the absence of an axion, including distortions arising from reduced dimensionality and finite-size effects. Upon coupling the system to a dynamical axion field, the vacuum energy relaxes to a minimum at $\theta_{\text{eff}} = 0$ and becomes nearly independent of the initial $\bar{\theta}$. These results demonstrate that the Peccei-Quinn mechanism can be realized in controlled, few-qubit quantum simulations, opening a new route to exploring topological gauge dynamics on quantum hardware.

Gauge-field Lagrangian to Hamiltonian. To express the QCD Lagrangian in a form suitable for canonical quantization, we rewrite the gluon field-strength tensor $G_{\mu\nu}^a$ in terms of its temporal and spatial components. In analogy to electromagnetism, we define the chromoelectric and chromomagnetic fields as

$$E_i^a = G_{0i}^a, \quad B_i^a = -\frac{1}{2}\epsilon_{ijk}G_{jk}^a, \quad (3)$$

where i, j, k denote spatial indices, and $a = 1, \dots, 8$ labels the color components of the $SU(3)$ gauge group.

Substituting these definitions into the gauge-field part of the QCD Lagrangian (1), i.e., $\mathcal{L}_{\text{gauge}} = -\frac{1}{4}G_{\mu\nu}^a G^{a,\mu\nu} + \bar{\theta}\frac{g^2}{32\pi^2}G_{\mu\nu}^a \tilde{G}^{a,\mu\nu}$, and using the identity $G_{\mu\nu}^a \tilde{G}^{a,\mu\nu} =$

$-4\mathbf{E}^a \cdot \mathbf{B}^a$, we obtain

$$\mathcal{L}_{\text{gauge}} = \frac{1}{2}\mathbf{E}^a \cdot \mathbf{E}^a - \frac{1}{2}\mathbf{B}^a \cdot \mathbf{B}^a + \bar{\theta}\frac{g^2}{8\pi^2}\mathbf{E}^a \cdot \mathbf{B}^a. \quad (4)$$

The first two terms represent the kinetic and potential energy densities of the gluon fields, respectively, while the last term introduces the coupling between the chromoelectric and chromomagnetic fields that violates CP symmetry.

The canonical momentum conjugate to the spatial gauge field A_i^a is given by

$$\Pi_i^a = \frac{\partial \mathcal{L}_{\text{gauge}}}{\partial(\partial_0 A_i^a)} = E_i^a + \bar{\theta}\frac{g^2}{8\pi^2}B_i^a, \quad (5)$$

showing that the $\bar{\theta}$ -term shifts the momentum by an amount proportional to the chromomagnetic field. This term couples the electric and magnetic sectors, thus Π_i^a no longer equals the electric field, and thereby modifying the canonical structure of the theory.

The Hamiltonian is then constructed via the Legendre transformation [18]

$$\begin{aligned} \mathcal{H}_{\text{gauge}} &= \Pi_i^a \partial_0 A_i^a - \mathcal{L}_{\text{gauge}} \\ &= \frac{1}{2}(\mathbf{E}^a \cdot \mathbf{E}^a + \mathbf{B}^a \cdot \mathbf{B}^a) - \bar{\theta}\frac{g^2}{8\pi^2}\mathbf{E}^a \cdot \mathbf{B}^a. \end{aligned} \quad (6)$$

Under charge conjugation C and parity P transformations, the chromoelectric and chromomagnetic fields transform as

$$\mathbf{E}^a \xrightarrow{P} -\mathbf{E}^a, \quad \mathbf{B}^a \xrightarrow{P} \mathbf{B}^a, \quad \mathbf{E}^a \xrightarrow{C} -\mathbf{E}^a, \quad \mathbf{B}^a \xrightarrow{C} -\mathbf{B}^a. \quad (7)$$

Therefore, the scalar product $\mathbf{E}^a \cdot \mathbf{B}^a$ is odd under both P and CP

$$\mathbf{E}^a \cdot \mathbf{B}^a \xrightarrow{CP} -\mathbf{E}^a \cdot \mathbf{B}^a. \quad (8)$$

Consequently, the term proportional to $\bar{\theta}\mathbf{E}^a \cdot \mathbf{B}^a$ in the Hamiltonian (6) explicitly breaks CP symmetry. Although small in magnitude (given experimental constraints on $\bar{\theta}$), this term could induce observable effects such as a permanent EDM in color-neutral hadrons like the neutron [7, 8].

Simplified (1+1)D $U(1)$ Schwinger model. We consider a (1+1)-dimensional Schwinger model, corresponding to one spatial and one temporal dimension [19, 20]. Despite its Abelian gauge structure, this model reproduces several nonperturbative features in QCD, including confinement of charges, a dynamically generated mass gap, and spontaneous chiral symmetry breaking in the massless limit [20–23]. It also possesses a nontrivial topological vacuum structure analogous to the $\bar{\theta}$ -vacua of QCD, allowing controlled investigations of CP -violating

effects induced by a background $\bar{\theta}$ -term in (1+1) dimensions [23, 24]. Crucially, the Schwinger model admits a well-defined lattice discretization and a finite-dimensional gauge-link formulation [25], making it ideally suited for implementation on quantum computing platforms [26].

In (1+1) dimensions, the gauge field has only one spatial component, and the magnetic field identically vanishes. The gauge-field dynamics are therefore governed by the electric field $E(x)$, which serves as the canonical conjugate to the spatial gauge potential $A_1(x)$. The commutation relation reads $[A_1(x), E(y)] = i\delta(x - y)$, analogous to that between position and momentum in quantum mechanics. The continuum Lagrangian for a single fermion flavor coupled to this Abelian gauge field, including the topological $\bar{\theta}$ -term, can be written as

$$\mathcal{L} = \bar{\psi}(i\gamma^\mu D_\mu - m)\psi - \frac{1}{2}E^2 + \frac{\bar{\theta}}{2\pi}E, \quad (9)$$

where the gauge-covariant derivative is $D_\mu = \partial_\mu - igA_\mu$. The Legendre transformation gives

$$H = \int dx \left[\psi^\dagger(x) \left(-i\gamma^1 D_1 + m\gamma^0 \right) \psi(x) + \frac{1}{2} \left(E(x) - \frac{\bar{\theta}}{2\pi} \right)^2 \right],$$

where the shift $E(x) \rightarrow E(x) - \frac{\bar{\theta}}{2\pi}$ encodes the CP -odd topological term. This structure is analogous to the **E**·**B** coupling in QCD but simpler in one spatial dimension.

For quantum simulation, we adopt the Kogut-Susskind lattice discretization [27, 28], with gauge links $U_{x,x+1} = e^{iA_{x,x+1}}$ and electric fields E_x . The discretized Hamiltonian reads

$$H = \frac{m}{2} \sum_x (-1)^x Z_x + w \sum_x (\psi_x^\dagger U_{x,x+1} \psi_{x+1} + \text{h.c.}) + \frac{g^2}{2} \sum_x \left(E_x - \frac{\bar{\theta}}{2\pi} \right)^2, \quad (10)$$

where $Z_x \equiv 1 - 2\psi_x^\dagger \psi_x$ denotes the local charge operator. The alternating sign $(-1)^x$ stems from the staggered-fermion scheme, which suppresses fermion doubling while preserving chiral symmetry.

To ensure gauge invariance, the Hamiltonian must satisfy Gauss's law at every lattice site. This constraint can be imposed dynamically by adding a large penalty term $\lambda \sum_x G_x^2$, where the generator of gauge transformations G_x is defined by

$$G_x = E_{x-1,x} - E_{x,x+1} - \psi_x^\dagger \psi_x + \eta_x. \quad (11)$$

The constant η_x represents a background charge determined by the staggering convention. Physical states of the theory obey $G_x|\text{phys}\rangle = 0$, ensuring local charge neutrality and gauge invariance.

Two sites lattice case. Restricting the system to its smallest nontrivial instance, i.e., two sites lattice connected by

a single link, yields the minimal Hamiltonian

$$H = \frac{m}{2}(-Z_0 + Z_1) + w(\psi_0^\dagger U_{01} \psi_1 + \text{h.c.}) + \frac{g^2}{2} \left(E - \frac{\bar{\theta}}{2\pi} \right)^2 + \lambda \sum_x G_x^2. \quad (12)$$

In this representation, the first term corresponds to the staggered mass energy, the second encodes gauge-invariant fermion hopping between the two sites mediated by the link operator U_{01} , and the third term represents the electric-field energy including the CP -violating $\bar{\theta}$ shift. The final term enforces Gauss's law through an energetic constraint, restricting the evolution to the gauge-invariant subspace.

This minimal Schwinger model retains the topological and CP -violating structure of the QCD Hamiltonian. The $\bar{\theta}$ -dependent electric-field shift plays the role of an effective CP -odd background field, allowing one to explore parity violation, vacuum degeneracy, and $\bar{\theta}$ -vacuum transitions within a low-dimensional analog of strong interactions.

To implement the model on quantum computers, both the fermionic and gauge degrees of freedom are encoded in qubits (spin- $\frac{1}{2}$ systems). The fermionic modes are mapped to qubits using the Jordan-Wigner (JW) transformation [29], which preserves the correct anticommutation relations through parity strings, and each gauge link is represented by a single qubit in the quantum-link formulation. The staggered fermion fields ψ_x and ψ_x^\dagger satisfy

$$\{\psi_x, \psi_y^\dagger\} = \delta_{xy}, \text{ and } \{\psi_x, \psi_y\} = 0. \quad (13)$$

In the JW representation, they are written as

$$\psi_x = \left(\prod_{y < x} Z_y \right) S_x^-, \text{ and } \psi_x^\dagger = \left(\prod_{y < x} Z_y \right) S_x^+, \quad (14)$$

where $S_x^\pm = (X_x \pm iY_x)/2$. The string $\prod_{y < x} Z_y$ enforces fermionic parity between sites. Here X , Y , and Z are Pauli matrices. The quantum-link representation of the gauge field is given by $E = (I - Z_\ell)/2$ and $U = (X_\ell + iY_\ell)/2$, where ℓ stands for the single-link qubit. See App. for the full derivation.

Substituting these mappings into Hamiltonian (12) yields an explicit expression in terms of Pauli matrices. The mass term, representing the energy cost of occupation on alternating sites due to the staggered fermion formulation, becomes

$$H_m = \frac{m}{2}(-Z_0 + Z_1). \quad (15)$$

The electric-field energy term, including the CP -

violating $\bar{\theta}$ -shift yields

$$\begin{aligned} H_{\bar{\theta}} &= \frac{g^2}{2} \left(E - \frac{\bar{\theta}}{2\pi} \right)^2 \\ &= \frac{g^2}{2} \left[\left(\frac{\bar{\theta}}{2\pi} \right)^2 - \frac{\bar{\theta}}{2\pi} + \frac{1}{2} \right] I_l + \frac{g^2}{2} \left(\frac{\bar{\theta}}{2\pi} - \frac{1}{2} \right) Z_\ell. \end{aligned} \quad (16)$$

The constant term merely shifts the global energy, while the Z_ℓ -dependent term changes sign at $\bar{\theta} = \pi$, leading to the correct 2π periodicity.

The fermion hopping term, which describes gauge-invariant tunneling between the two sites, takes the form

$$\begin{aligned} H_{\text{hop}} &= w \left(\psi_0^\dagger U_{01} \psi_1 + \psi_1^\dagger U_{01}^\dagger \psi_0 \right) \\ &= \frac{w}{8} (X_0 X_1 X_\ell + Y_0 Y_1 X_\ell - X_0 Y_1 Y_\ell - Y_0 X_1 Y_\ell), \end{aligned} \quad (17)$$

which consists of three-body Pauli interactions coupling the two fermionic qubits with the gauge-field qubit. These terms correspond to correlated hopping processes in which a fermion moves between sites 0 and 1 while simultaneously changing the electric flux on the link, thus preserving local gauge invariance.

Finally, Gauss's law is imposed through an energy penalty term that ensures the dynamics remain confined to the gauge-invariant subspace. In Pauli form, this constraint is represented by

$$H_G = \lambda \sum_x G_x^2 = \lambda \left(\sum_{i=0,1,\ell} c_i Z_i + \sum_{i=0}^1 d_{i\ell} Z_i Z_\ell \right), \quad (18)$$

where the coefficients $c_i, d_{i\ell} \in \{\pm \frac{1}{2}\}$ are fixed by the staggering and boundary conditions. A large $\lambda \gg \max(m, w, g^2)$ suppresses gauge-violating excitations and confines the dynamics to the physical subspace satisfying $G_x |\text{phys}\rangle = 0$.

Combining all contributions, the total effective Hamiltonian for the two-site Schwinger model reaches

$$H_{\text{total}} = H_m + H_{\text{hop}} + H_{\bar{\theta}} + H_G. \quad (19)$$

Despite its simplicity, this model retains the nontrivial topological and CP -violating structure of QCD and provides an ideal platform for near-term quantum simulations of gauge-theory dynamics.

The Peccei-Quinn mechanism. To dynamically relax the CP -violating angle, we promote the parameter $\bar{\theta}$ to a dynamical variable by introducing an axion field $a(x)$ with decay constant f_a . At low energies, the effective QCD-axion Lagrangian is

$$\mathcal{L}_{\text{QCD+a}} = \mathcal{L}_{\text{QCD}} \Big|_{\bar{\theta} \rightarrow \bar{\theta} + \frac{a}{f_a}} + \frac{1}{2} \partial_\mu a \partial^\mu a - V \left(\bar{\theta} + \frac{a}{f_a} \right). \quad (20)$$

Model	w	g^2	m	λ	Gauss-law	Axion
Near-continuum	1	1	0.25	40	$c_0 = -\frac{1}{2},$ $c_1 = \frac{1}{2},$ $c_\ell = 0,$	$m_a = g^2,$ $f_a = 2$
Balanced benchmark	1	2	0.25	40		
Strong gauge coupling	1	5	0.25	40	$d_{0\ell} = d_{1\ell} = -\frac{1}{2}$	

TABLE I. **Parameter sets used in numerical simulations.** The Gauss-law and axion parameters are used for all models.

The axion enters as a shift of the effective CP -violating angle, $\theta_{\text{eff}} \equiv \bar{\theta} + a/f_a$, rendering it dynamical.

At energies below the QCD confinement scale, the axion potential is well described in a model-independent way by the topological susceptibility χ ,

$$V(\theta_{\text{eff}}) \simeq \chi [1 - \cos(\theta_{\text{eff}})]. \quad (21)$$

Expanding around the minimum yields the standard axion mass relation $m_a^2 f_a^2 = \chi$.

The axion Hamiltonian density follows from the canonical momentum $\pi_a = \dot{a}$ and is given by

$$\mathcal{H}_a = \frac{1}{2} \pi_a^2 + \frac{1}{2} (\partial_x a)^2 + V(\theta_{\text{eff}}), \quad (22)$$

with the total axion Hamiltonian $H_a = \int dx \mathcal{H}_a$. The coupling between the axion and the gauge sector appears through the shifted $\bar{\theta}$ term,

$$H_{\bar{\theta}+a} = \frac{g^2}{2} \left(E - \frac{\theta_{\text{eff}}}{2\pi} \right)^2. \quad (23)$$

Combining all contributions, the full Hamiltonian of the axion-coupled system reads

$$H_{\text{total}} = H_m + H_{\text{hop}} + H_{\bar{\theta}+a} + H_a + H_G. \quad (24)$$

The axion dynamics drive the system toward the minimum of the effective potential. Minimization with respect to a enforces $\langle a \rangle = -f_a \bar{\theta}$, so that the effective angle relaxes to $\theta_{\text{eff}} = 0$. This realizes the Peccei-Quinn mechanism at the Hamiltonian level: the axion back-reaction dynamically cancels the CP -violating phase, restoring a CP -symmetric vacuum.

Numerical simulation. We compute the ground state of the two-site Schwinger-model Hamiltonian in its qubit representation using the feedback-based FALQON algorithm [17]. FALQON updates the control parameters in real time to ensure a strictly monotonic decrease of the energy expectation value, enabling ground-state preparation without any classical optimization loop. See detail of FALQON in App. .

We evaluate the resulting states across different parameter regimes to examine confinement and CP -violating effects. For benchmarking and calibration, we focus on three representative configurations:

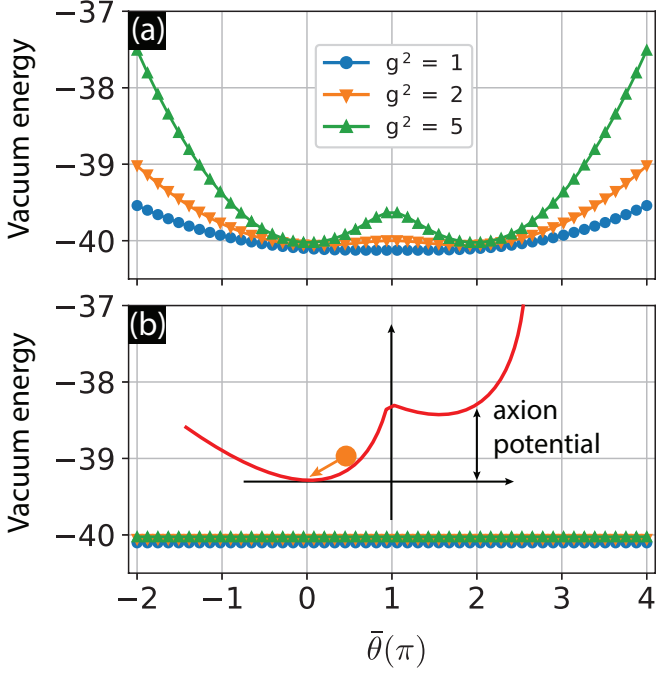


FIG. 1. **Vacuum energy of the two-site lattice Schwinger model with and without a dynamical axion.** (a) Vacuum energy $E_0(\bar{\theta})$ as a function of $\bar{\theta}$ for three representative parameter regimes. In the $(1+1)$ -dimensional lattice formulation, reduced dimensionality and discretization effects lift intermediate branches, such that only the minima at $\bar{\theta} = 0$ and 2π are clearly resolved. (b) Vacuum energy after coupling to a dynamical axion field. The axion back-reaction drives the effective angle $\theta_{\text{eff}} = \bar{\theta} + a/f_a$ toward zero, rendering E_0 independent of $\bar{\theta}$. *Inset:* Schematic axion-induced effective potential illustrating the relaxation of θ_{eff} toward its global minimum.

1. **Near-continuum:** $w = 1$, $g^2 = 1$, $m = 0.25$, and $\lambda = 40$. In this limit, the system approaches the weak-coupling or near-continuum regime. Increasing the ratio w/g (i.e., decreasing g) allows one to track how the ground-state energy and charge distribution evolve with reduced discretization effects.
2. **Balanced benchmark:** $w = 1$, $g^2 = 2$, $m = 0.25$, and $\lambda = 40$. This choice provides a well-balanced regime where fermionic tunneling, gauge energy, and mass terms contribute comparably, yielding a nontrivial but numerically stable energy spectrum.
3. **Strong gauge coupling:** $w = 1$, $g^2 = 5$, $m = 0.25$, and $\lambda = 40$. Increasing g^2 amplifies the electric-field contribution to the energy, which reduces charge fluctuations and favors configurations with minimal local net charge.

For the Gauss-law constraint, we use $c_0 = -\frac{1}{2}$, $c_1 = \frac{1}{2}$, $c_\ell = 0$, $d_{0\ell} = d_{1\ell} = -\frac{1}{2}$. For the axion sector, we set m_a and f_a to be comparable to the gauge-field energy

scale, choosing $m_a = g^2$, $f_a = 2$. The full parameter set is summarized in Tab. I.

Fig. 1 (a) shows the vacuum energy $E_0(\bar{\theta})$ as a function $\bar{\theta}$ (in units of π) for three representative parameter regimes: near-continuum, balanced benchmark, and strong gauge coupling, in the absence of an axion field [Hamiltonian Eq. (19)]. In the continuum QCD, $E_0(\bar{\theta})$ is expected to be a 2π -periodic function of $\bar{\theta}$, with degenerate minima at $\bar{\theta} = 0$ (mod 2π). In the present $(1+1)$ -dimensional Schwinger-model approximation, lattice discretization, reduced dimensionality, and strong-coupling effects distort this periodic structure. Consequently, only the minima at $\bar{\theta} = 0$ and 2π are clearly resolved, while intermediate branches are lifted. This distortion becomes more pronounced at stronger gauge coupling, where the vacuum energy exhibits a steeper curvature away from the minima.

Fig. 1 (b) illustrates the effect of coupling the system to a dynamical axion field. Starting from a generic initial value of $\bar{\theta}$, the axion dynamically relaxes toward the minimum of the combined potential, driving the effective angle $\theta_{\text{eff}} = \bar{\theta} + a/f_a$ toward zero. As a result, the relaxed vacuum energies become independent of $\bar{\theta}$, demonstrating the dynamical cancellation of CP violation. The inset schematically illustrates the axion-induced effective potential as a function of $\bar{\theta}$, where the axion field shifts θ_{eff} toward the global minimum. Despite dimensional and lattice artifacts inherent to the $(1+1)$ D formulation, these results confirm that the Peccei-Quinn mechanism remains operative at the Hamiltonian level.

Extended lattice: 4 sites and 3 links (7 qubits). Figure 2 summarizes the ground-state energy landscape of the qubit-encoded Schwinger model extended to a four-site lattice with three gauge links. The explicit Hamiltonian, including mass, gauge-mediated hopping, electric-field energy, and Gauss-law terms, is given in App. . As in Fig. 1, we evaluate the vacuum energy $E_0(\bar{\theta})$ for three representative parameter regimes: near-continuum (blue), balanced benchmark (orange), and strong gauge coupling (green).

Figure 2(a) shows the case without the axion field. Similar to the two-site case shown in Fig. 1(a), the vacuum energy exhibits minima at $\bar{\theta} = 0$ and 2π . In the enlarged lattice, the increased number of gauge-link degrees of freedom modifies the electric-field distribution, leading to finite-volume effects that distort the ideal continuum periodic structure. As a result, the vacuum does not exhibit a fully resolved 2π -periodic landscape, and intermediate branches are lifted relative to the minima.

Figure 2(b) displays the same model after coupling to a dynamical axion. As in Fig. 1(b), the axion dynamically shifts the effective angle $\bar{\theta} \rightarrow \theta_{\text{eff}} = \bar{\theta} + a/f_a$ and introduces a restoring potential. After relaxation, the vacuum energy becomes independent of $\bar{\theta}$, with the global minimum driven to $\theta_{\text{eff}} = 0$ for all parameter regimes. This behavior demonstrates that the Peccei-Quinn mechanism

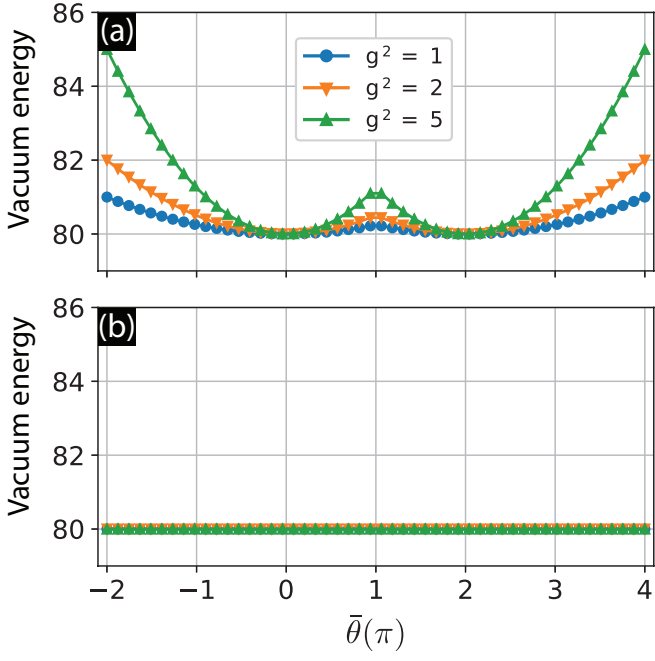


FIG. 2. **Vacuum energy of the four sites lattice Schwinger model with and without a dynamical axion.** Vacuum energy $E_0(\bar{\theta})$ of the qubit-encoded Schwinger model for three representative parameter regimes, shown using the same conventions as Fig. 1 for (a) without axion field, and (b) with axion field.

remains operative and robust against finite-volume effects, restoring a CP -symmetric vacuum even in an enlarged lattice realization implemented with seven qubits.

Conclusion. Starting from the QCD Lagrangian with a CP -violating $\bar{\theta}$ term, we derived the corresponding Hamiltonian and identified how this term modifies the gauge-sector structure. By reducing the theory to its $(1+1)$ -dimensional Schwinger-model analogue, we obtained a minimal setting that preserves essential nonperturbative features, including topological vacuum structure and sensitivity to $\bar{\theta}$. Using Jordan-Wigner and quantum-link mappings, the model was rewritten as an explicit Pauli Hamiltonian suitable for digital quantum simulation. We evaluated the ground state using the FALQON algorithm and computed the vacuum energy as a function of $\bar{\theta}$, reproducing the expected vacuum behavior of a theory with a CP -violating term. Upon coupling the system to a dynamical axion field, the vacuum energy relaxes to a minimum at $\theta_{\text{eff}} = 0$, demonstrating the dynamical cancellation of CP violation. These results provide a concrete quantum-simulation realization of the Peccei-Quinn mechanism and establish a controlled platform for studying CP violation and its dynamical relaxation in gauge theories.

Acknowledgments. This work is supported by the Tohoku Initiative for Fostering Global Researchers for Interdisciplinary Sciences (TI-FRIS) of MEXT's Strategic Profes-

sional Development Program for Young Researchers.

Data availability. No data were created or analyzed in this study.

Appendix A: Jordan-Wigner Transformation

To simulate the $(1+1)$ D lattice Schwinger model on a quantum computer, the Hamiltonian must be expressed entirely in terms of Pauli matrices acting on qubits. This requires mapping both the fermionic matter fields and the gauge link variables to spin- $\frac{1}{2}$ operators. The fermionic fields are encoded using the Jordan-Wigner (JW) transformation, while the gauge links are represented by spin operators in the quantum link model (QLM), which provides a finite-dimensional truncation of the continuous gauge degrees of freedom.

The staggered fermion fields ψ_x and ψ_x^\dagger satisfy canonical anticommutation relations

$$\{\psi_x, \psi_y^\dagger\} = \delta_{xy}, \quad \{\psi_x, \psi_y\} = 0.$$

In the JW representation, these operators are mapped to Pauli operators on a chain of qubits as

$$\psi_x = \left(\prod_{y < x} Z_y \right) S_x^-, \quad \psi_x^\dagger = \left(\prod_{y < x} Z_y \right) S_x^+, \quad (25)$$

where $S_x^\pm = (X_x \pm iY_x)/2$ are the ladder operators, and the string $\prod_{y < x} Z_y$ encodes fermionic parity to ensure the correct anticommutation between different sites. For the minimal two-site model ($x = 0, 1$), this reduces to

$$\psi_0 = S_0^-, \quad \psi_0^\dagger = S_0^+, \quad \psi_1 = Z_0 S_1^-, \quad \psi_1^\dagger = Z_0 S_1^+. \quad (26)$$

Each qubit represents one fermionic site, with the computational basis states $|0\rangle$ and $|1\rangle$ corresponding respectively to the unoccupied and occupied fermion configurations.

The gauge field on the link connecting sites 0 and 1 is represented by a third qubit. We denote the link qubit is ℓ . In the QLM formulation, the electric field and link operators are encoded as

$$E = \frac{I - Z_\ell}{2}, \quad U_{01} = \frac{X_\ell + iY_\ell}{2}, \quad U_{01}^\dagger = \frac{X_\ell - iY_\ell}{2}. \quad (27)$$

Here, E measures the quantized electric flux on the link, while U_{01} and U_{01}^\dagger act as raising and lowering operators for the electric field, satisfying $[E, U_{01}] = U_{01}$ and $[E, U_{01}^\dagger] = -U_{01}^\dagger$. The eigenvalues of Z_ℓ correspond to discrete electric-field strengths $E \in \{0, 1\}$, providing the simplest nontrivial truncation of the gauge degree of freedom.

Substituting these mappings into the continuum lattice Hamiltonian yields a fully qubit-based representation. The staggered-mass term, which alternates in sign

to reproduce chiral symmetry in the continuum limit, becomes

$$H_m = \frac{m}{2}(-Z_0 + Z_1). \quad (28)$$

The electric-field energy, including the $\bar{\theta}$ -dependent CP -violating shift, takes the form

$$\begin{aligned} H_{\bar{\theta}} &= \frac{g^2}{2} \left(E - \frac{\bar{\theta}}{2\pi} \right)^2 \\ &= \frac{g^2}{2} \left[\left(\frac{\bar{\theta}}{2\pi} \right)^2 - \frac{\bar{\theta}}{2\pi} + \frac{1}{2} \right] I_{\ell} + \frac{g^2}{2} \left(\frac{\bar{\theta}}{2\pi} - \frac{1}{2} \right) Z_{\ell}. \end{aligned} \quad (29)$$

The gauge-invariant hopping term is given by

$$\begin{aligned} H_{\text{hop}} &= w(\psi_0^\dagger U_{01} \psi_1 + \psi_1^\dagger U_{01}^\dagger \psi_0) \\ &= \frac{w}{8} (X_0 X_1 X_{\ell} + Y_0 Y_1 X_{\ell} - X_0 Y_1 Y_{\ell} - Y_0 X_1 Y_{\ell}), \end{aligned} \quad (30)$$

which involves correlated three-body interactions between the two matter qubits and the gauge-link qubit, ensuring local gauge invariance. Local charge conservation is imposed energetically through a penalty term

$$H_G = \lambda \sum_x G_x^2 = \lambda \left(\sum_{i=0,1,\ell} c_i Z_i + \sum_{i=0}^1 d_{i\ell} Z_i Z_{\ell} \right), \quad (31)$$

where G_x is the Gauss-law generator and the coefficients $c_i, d_{i\ell} \in \{\pm \frac{1}{2}\}$ are fixed by the staggering and boundary conditions.

Combining all contributions gives the complete two-site Pauli Hamiltonian,

$$H_{\text{total}} = H_m + H_{\text{hop}} + H_{\bar{\theta}} + H_G, \quad (32)$$

where H_m encodes the fermionic mass asymmetry, H_{hop} the correlated fermion-gauge tunneling, $H_{\bar{\theta}}$ the CP -violating electric-field shift, and H_G enforces gauge invariance. Despite its minimal size, this model captures essential features of the Schwinger mechanism and provides a compact benchmark for near-term quantum simulations of gauge-theory dynamics.

Appendix B: Ground-state preparation via FALQON

To obtain the ground state of the lattice Schwinger Hamiltonian, we employ the Feedback-based Algorithm for Quantum Optimization (FALQON) [17]. FALQON formulates the search for the ground state as a closed-loop quantum control problem. The system evolves under a time-dependent Hamiltonian composed of a cost term H_C (the problem Hamiltonian) and a driver term H_D that induces state transitions:

$$H(t) = H_C + \beta(t) H_D, \quad (33)$$

where $\beta(t)$ is a feedback control field updated at each iteration according to

$$\beta(t) = -\langle \psi(t) | i[H_D, H_C] | \psi(t) \rangle. \quad (34)$$

This choice guarantees that the expectation value of the cost energy decreases monotonically,

$$\frac{d}{dt} \langle H_C \rangle_t = -i |\langle [H_D, H_C] \rangle_t|^2 \leq 0, \quad (35)$$

ensuring convergence toward the ground state without classical optimization loops.

In discrete time, the evolution is implemented by a sequence of p alternating unitaries,

$$|\psi_{k+1}\rangle = e^{-i\Delta t \beta_k H_D} e^{-i\Delta t H_C} |\psi_k\rangle, \quad (36)$$

$$\beta_{k+1} = -\langle \psi_k | i[H_D, H_C] | \psi_k \rangle, \quad (37)$$

with time step Δt . In our simulations, we set $H_C = H_{\text{total}}$ as the full Schwinger-model Hamiltonian and choose $H_D = \sum_i X_i$ as a global mixer acting on all qubits. The FALQON feedback mechanism automatically tunes the control amplitudes $\{\beta_k\}$ to minimize the system energy, yielding efficient and noise-robust ground-state convergence compared with traditional variational algorithms.

Appendix C: Four sites and three links (7 qubits) model

We consider a four-site open chain with three gauge links. Matter (staggered) sites are $x = 0, 1, 2, 3$ and links are $\ell = 4, 5, 6$ connecting $(x, x+1)$. In a spin- $\frac{1}{2}$ quantum link model,

$$E_{\ell} = \frac{I - Z_{\ell}}{2}, \quad U_{\ell} = \frac{1}{2}(X_{\ell} + iY_{\ell}). \quad (38)$$

With JW fermions, we use

$$\text{matter qubits: } q_0, q_1, q_2, q_3 \leftrightarrow x = 0, 1, 2, 3, \quad (39)$$

$$\text{link qubits: } q_4, q_5, q_6 \leftrightarrow \ell = 4, 5, 6. \quad (40)$$

The total Hamiltonian is

$$H = H_m + H_{\text{hop}} + H_{\bar{\theta}} + H_G + \text{const.} \quad (41)$$

First, the mass term with the standard staggered sign

$$H_m = \frac{m}{2} (-Z_{q_0} + Z_{q_1} - Z_{q_2} + Z_{q_3}). \quad (42)$$

For the Gauge electric energy with $\bar{\theta}$ -term, using the shifted quadratic form

$$H_{\bar{\theta}} = \frac{g^2}{2} \sum_{\ell=4}^6 \left(E_{\ell} - \frac{\bar{\theta}}{2\pi} \right)^2, \quad E_{\ell} = \frac{I - Z_{q_{\ell}}}{2}. \quad (43)$$

For the Gauge-invariant hopping, with JW strings, we have $\psi_x = (\prod_{y < x} Z_{q_y}) \sigma_{q_x}^-$ and link $U_{\ell=x+4}$ on $(x, x+1)$, the cancellations yield

$$\begin{aligned} H_{\text{hop}} &= w \sum_{x=0}^2 (\psi_x^\dagger U_x \psi_{x+1} + \text{h.c.}) \\ &= \frac{w}{8} \sum_{x=0}^2 \left(X_{q_x} X_{q_{x+1}} X_{q_\ell} + Y_{q_x} Y_{q_{x+1}} X_{q_\ell} - \right. \\ &\quad \left. X_{q_x} Y_{q_{x+1}} Y_{q_\ell} - Y_{q_x} X_{q_{x+1}} Y_{q_\ell} \right). \quad (44) \end{aligned}$$

For Gauss's law and penalty, with open boundaries,

$$G_x = E_{x-1,x} - E_{x,x+1} - (n_x - \eta_x), \quad (45)$$

$$n_x = \frac{I - Z_{q_x}}{2}, \quad (46)$$

$$\eta_x = -\frac{1}{2}[1 - (-1)^x], \quad (47)$$

with $E_{-1,0} = E_{3,4} = 0$. We enforce gauge invariance via a large penalty and get

$$H_G = \lambda \sum_{x=0}^3 G_x^2, \quad \lambda \gg \max(m, w, g^2). \quad (48)$$

—

* Electronic address: binho@fris.tohoku.ac.jp

- [1] G. 't Hooft, Quantum chromodynamics, *Annalen der Physik* **512**, 925 (2000).
- [2] F. Gross, E. Klemp, S. J. Brodsky, A. J. Buras, V. D. Burkert, G. Heinrich, K. Jakobs, C. A. Meyer, K. Orginos, M. Strickland, J. Stachel, G. Zanderighi, N. Brambilla, P. Braun-Munzinger, D. Britzger, S. Capstick, T. Cohen, V. Crede, M. Constantinou, C. Davies, L. Del Debbio, A. Denig, C. DeTar, A. Deur, Y. Dokshitzer, H. G. Dosch, J. Dudek, M. Dunford, E. Epelbaum, M. A. Escobedo, H. Fritzsch, K. Fukushima, P. Gambino, D. Gillberg, S. Gottlieb, P. Grafstrom, M. Grazzini, B. Grube, A. Guskov, T. Iijima, X. Ji, F. Karsch, S. Kluth, J. B. Kogut, F. Krauss, S. Kumanou, D. Leinweber, H. Leutwyler, H.-B. Li, Y. Li, B. Malaescu, C. Mariotti, P. Maris, S. Marzani, W. Melnitchouk, J. Messchendorp, H. Meyer, R. E. Mitchell, C. Mondal, F. Nerling, S. Neubert, M. Pappagallo, S. Pastore, J. R. Peláez, A. Puckett, J. Qiu, K. Rabbertz, A. Ramos, P. Rossi, A. Rustamov, A. Schäfer, S. Scherer, M. Schindler, S. Schramm, M. Shifman, E. Shuryak, T. Sjöstrand, G. Sterman, I. W. Stewart, J. Stroth, E. Swanson, G. F. de Téramond, U. Thoma, A. Vairo, D. van Dyk, J. Vary, J. Virto, M. Vos, C. Weiss, M. Wobisch, S. L. Wu, C. Young, F. Yuan, X. Zhao, and X. Zhou, 50 years of quantum chromodynamics, *The European Physical Journal C* **83**, 1125 (2023).
- [3] A. A. A. Likéné, D. N. Ongodo, P. M. Tsila, A. Atangana, and G. H. Ben-Bolie, Quantum chromodynamics lagrangian density and $\text{su}(3)$ gauge symmetry: A fractional approach, *Modern Physics Letters A* **39**, 2450194 (2024).
- [4] G. 't Hooft, Symmetry breaking through bell-jackiw anomalies, *Phys. Rev. Lett.* **37**, 8 (1976).
- [5] G. 't Hooft, Computation of the quantum effects due to a four-dimensional pseudoparticle, *Phys. Rev. D* **14**, 3432 (1976).
- [6] J. E. Kim and G. Carosi, Axions and the strong cp problem, *Rev. Mod. Phys.* **82**, 557 (2010).
- [7] R. Crewther, P. Di Vecchia, G. Veneziano, and E. Witten, Chiral estimate of the electric dipole moment of the neutron in quantum chromodynamics, *Physics Letters B* **88**, 123 (1979).
- [8] M. Pospelov and A. Ritz, Electric dipole moments as probes of new physics, *Annals of Physics* **318**, 119 (2005), special Issue.
- [9] C. A. Baker, D. D. Doyle, P. Geltenbort, K. Green, M. G. D. van der Grinten, P. G. Harris, P. Iaydjiev, S. N. Ivanov, D. J. R. May, J. M. Pendlebury, J. D. Richardson, D. Shiers, and K. F. Smith, Improved experimental limit on the electric dipole moment of the neutron, *Phys. Rev. Lett.* **97**, 131801 (2006).
- [10] C. Abel, S. Afach, N. J. Ayres, C. A. Baker, G. Ban, G. Bison, K. Bodek, V. Bondar, M. Burghoff, E. Chanel, Z. Chowdhuri, P.-J. Chiu, B. Clement, C. B. Crawford, M. Daum, S. Emmenegger, L. Ferraris-Bouchez, M. Fertl, P. Flaux, B. Franke, A. Fratangelo, P. Geltenbort, K. Green, W. C. Griffith, M. van der Grinten, Z. D. Grujić, P. G. Harris, L. Hayen, W. Heil, R. Henneck, V. Hélaine, N. Hild, Z. Hodge, M. Horras, P. Iaydjiev, S. N. Ivanov, M. Kasprzak, Y. Kermaidic, K. Kirch, A. Knecht, P. Knowles, H.-C. Koch, P. A. Koss, S. Komposch, A. Kozela, A. Kraft, J. Krempel, M. Kuźniak, B. Lauss, T. Lefort, Y. Lemière, A. Leredde, P. Mohanmurthy, A. Mtchedlishvili, M. Musgrave, O. Naviliat-Cuncic, D. Pais, F. M. Piegsa, E. Pierre, G. Pignol, C. Plonka-Spehr, P. N. Prashanth, G. Quéméner, M. Rawlik, D. Rebreyend, I. Rienäcker, D. Ries, S. Rocca, G. Rogel, D. Rozpedzik, A. Schnabel, P. Schmidt-Wellenburg, N. Severijns, D. Shiers, R. Tavakoli Dinani, J. A. Thorne, R. Virot, J. Voigt, A. Weis, E. Wursten, G. Wyszynski, J. Zejma, J. Zenner, and G. Zsigmond, Measurement of the permanent electric dipole moment of the neutron, *Phys. Rev. Lett.* **124**, 081803 (2020).
- [11] R. D. Peccei and H. R. Quinn, CP conservation in the presence of pseudoparticles, *Phys. Rev. Lett.* **38**, 1440 (1977).
- [12] R. D. Peccei and H. R. Quinn, Constraints imposed by CP conservation in the presence of pseudoparticles, *Phys. Rev. D* **16**, 1791 (1977).
- [13] R. D. Peccei, The strong cp problem and axions, in *Axions: Theory, Cosmology, and Experimental Searches*, edited by M. Kuster, G. Raffelt, and B. Beltrán (Springer Berlin Heidelberg, Berlin, Heidelberg, 2008) pp. 3–17.
- [14] F. Chadha-Day, J. Ellis, and D. J. E. Marsh, Axion dark matter: What is it and why now?, *Science Advances* **8**, eabj3618 (2022), <https://www.science.org/doi/pdf/10.1126/sciadv.abj3618>.
- [15] C. W. Bauer, Z. Davoudi, A. B. Balantekin, T. Bhattacharya, M. Carena, W. A. de Jong, P. Draper, A. El-Khadra, N. Gemelke, M. Hanada, D. Kharzeev, H. Lamm, Y.-Y. Li, J. Liu, M. Lukin, Y. Meurice, C. Monroe, B. Nachman, G. Pagano, J. Preskill, E. Rinaldi, A. Roggero, D. I. Santiago, M. J. Savage, I. Siddiqi, G. Siopsis, D. Van Zanten, N. Wiebe, Y. Yamauchi, K. Yeter-Aydeniz, and

S. Zorzetti, Quantum simulation for high-energy physics, *PRX Quantum* **4**, 027001 (2023).

[16] A. Di Meglio, K. Jansen, I. Tavernelli, C. Alexandrou, S. Arunachalam, C. W. Bauer, K. Borras, S. Carrazza, A. Crippa, V. Croft, R. de Putter, A. Delgado, V. Dunjko, D. J. Egger, E. Fernández-Combarro, E. Fuchs, L. Funcke, D. González-Cuadra, M. Grossi, J. C. Halimeh, Z. Holmes, S. Kühn, D. Lacroix, R. Lewis, D. Lucchesi, M. L. Martínez, F. Meloni, A. Mezzacapo, S. Montangero, L. Nagano, V. R. Pascuzzi, V. Radescu, E. R. Ortega, A. Roggero, J. Schuhmacher, J. Seixas, P. Silvi, P. Spentzouris, F. Tacchino, K. Temme, K. Terashi, J. Tura, C. Tüysüz, S. Vallecorsa, U.-J. Wiese, S. Yoo, and J. Zhang, Quantum computing for high-energy physics: State of the art and challenges, *PRX Quantum* **5**, 037001 (2024).

[17] A. B. Magann, K. M. Rudinger, M. D. Grace, and M. Sarovar, Feedback-based quantum optimization, *Phys. Rev. Lett.* **129**, 250502 (2022).

[18] R. K. P. Zia, E. F. Redish, and S. R. McKay, Making sense of the legendre transform, *American Journal of Physics* **77**, 614 (2009).

[19] K. Aoki and T. Ichihara, (1+1)-dimensional qcd with fundamental bosons and fermions, *Phys. Rev. D* **52**, 6435 (1995).

[20] J. Schwinger, Gauge invariance and mass. ii, *Phys. Rev.* **128**, 2425 (1962).

[21] X. Luo, Spontaneous chiral-symmetry breaking of lattice qcd with massless dynamical quarks, *Science in China Series G: Physics, Mechanics and Astronomy* **50**, 6 (2007).

[22] A. Ballon-Bayona, L. A. H. Mamani, and D. M. Rodrigues, Spontaneous chiral symme-try breaking in holographic soft wall models, *Phys. Rev. D* **104**, 126029 (2021).

[23] L. Funcke, K. Jansen, and S. Kühn, Topological vacuum structure of the schwinger model with matrix product states, *Phys. Rev. D* **101**, 054507 (2020).

[24] A. V. Smilga, Vacuum fields in the schwinger model, *Phys. Rev. D* **46**, 5598 (1992).

[25] G. Calliari, M. Di Liberto, H. Pichler, and T. V. Zache, Quantum simulating continuum field theories with large-spin lattice models, *PRX Quantum* **6**, 030304 (2025).

[26] E. Altman, K. R. Brown, G. Carleo, L. D. Carr, E. Demler, C. Chin, B. DeMarco, S. E. Economou, M. A. Eriksson, K.-M. C. Fu, M. Greiner, K. R. Hazzard, R. G. Hulet, A. J. Kollár, B. L. Lev, M. D. Lukin, R. Ma, X. Mi, S. Misra, C. Monroe, K. Murch, Z. Nazario, K.-K. Ni, A. C. Potter, P. Roushan, M. Saffman, M. Schleier-Smith, I. Siddiqi, R. Simmonds, M. Singh, I. Spielman, K. Temme, D. S. Weiss, J. Vučković, V. Vuletić, J. Ye, and M. Zwierlein, Quantum simulators: Architectures and opportunities, *PRX Quantum* **2**, 017003 (2021).

[27] J. Kogut and L. Susskind, Hamiltonian formulation of wilson's lattice gauge theories, *Phys. Rev. D* **11**, 395 (1975).

[28] E. Zohar and M. Burrello, Formulation of lattice gauge theories for quantum simulations, *Phys. Rev. D* **91**, 054506 (2015).

[29] P. Jordan and E. Wigner, Über das paulische äquivalenzverbot, *Zeitschrift für Physik* **47**, 631 (1928).